Extended π conjugation in 2*H*-1,4,2-diazaphosphole complexes†‡

Holger Helten,[a] Jörg Daniels,[a] Martin Nieger[b] and Rainer Streubel*[a]

Received (in Montpellier, France) 24th February 2010, Accepted 13th April 2010
DOI: 10.1039/c0nj00151a

Thienyl substituted 2*H*-1,4,2-diazaphosphole complexes **3a,b** were prepared *via* highly selective ring-expansion reactions of 2*H*-azaphosphirene complex **1** and nitriles with our new synthetic protocol using triflic acid and NEt_3. The single-crystal X-ray structures of **3a,b** show that the 3,5-substituents adopt a coplanar arrangement with the diazaphosphole ring resulting in extended π-conjugation, thus giving rise to absorptions at long wavelengths in their UV/Vis spectra. On the basis of Time-Dependent DFT (TD-DFT) calculations the longest-wavelength absorption could be assigned to a metal–ligand charge transfer (MLCT) process and another low-energy band was interpreted as a superposition of π–π* and n–π* transitions. Protonation of the ring nitrogen yields a pronounced bathochromic shift of all bands along with an increase in their intensity. These effects can be explained by the different extent to which the orbital energies are affected by protonation.

Introduction

Organic oligomers and polymers with a planar, π-conjugated backbone[1–25] have attracted considerable interest owing to their potential application in electronic devices such as organic light-emitting diodes (OLEDs),[2] field-effect transistors (FETs),[3] photovoltaic cells[4] and non-linear optical (NLO) devices.[5] With the view to developing novel frameworks with enhanced performance several strategies have been devised. One successful approach was to incorporate heterocyclic building blocks with different electronic nature in the π-conjugated backbone, whereby the optical and electronic properties of the materials could effectively be varied.[6–25] Enhanced conjugation due to intramolecular charge transfer (ICT) was reached in copolymers with alternating electron-rich and electron-deficient subunits, whereas it turned out that the effect is maximized through incorporation of heterocycles with low aromaticity.[7] For such purposes, *e.g.*, group-14 heterocyclopentadienes have extensively been employed.[8,9]

Réau and coworkers have established 2,5-diaryl- and 2,5-dihetaryl-phospholes **I** (Scheme 1),[10–19] and oligomers and polymers thereof have also been reported.[12–17] Thorough investigations on the optical and electrochemical properties of **I** revealed that delocalization of the π system reaches a maximum with two 2-thienyl substituents being attached in 2- and 5-position to the phosphole ring.[14] It was further

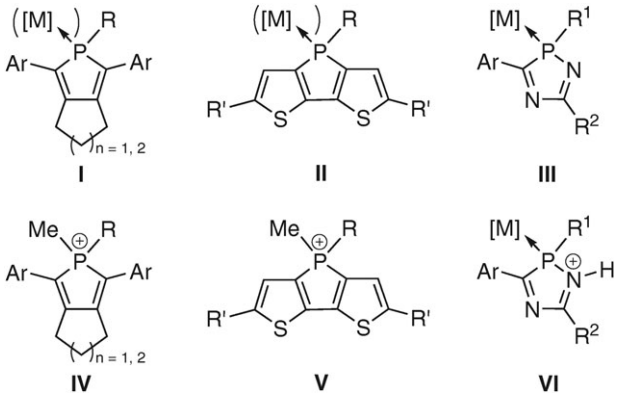

Scheme 1 Phospholes and complexes thereof **I**, **II**, 2*H*-1,4,2-diazaphosphole complexes **III**, phospholium ions **IV**, **V** and 2*H*-1,4,2-diazaphospholium ions **VI**.

supported by quantum chemical calculations that this effect is due to a low-lying LUMO, mainly localized at the phosphole moiety, in combination with a high HOMO energy caused by the electron-rich 2-thienyl substituents.[14] Thienyl groups have the further advantage that they are easily functionalized.[20] The properties of **I** can also be adjusted by modification at phosphorus, *e.g.*, by transition metal coordination.[13–18] Baumgartner and coworkers have developed a similar strategy making use of fused tricyclic dithieno[3,2-*b*:2′,3′-*d*]phospholes **II**.[11,21–25] Polymeric materials based on these systems have also been described.[21–23] The photophysical properties of **II** can effectively be tuned through variation of the substituents R at the thiophene rings or by modification at phosphorus. For example, complexation of the phosphorus center of derivatives of **II** with transition metal fragments such as AuCl or $W(CO)_5$ caused red shifts of the π–π* absorption by 20–50 nm.[24] It is noteworthy that pronounced bathochromic shifts were also observed upon *P*-alkylation of both **I**[14,16] and **II**[22] with methyl triflate giving **IV** and **V**, respectively. This effect was attributed to a lowering of the LUMO energy, and thus a lowering of the

[a] *Institut für Anorganische Chemie der Rheinischen Friedrich-Wilhelms-Universität Bonn, Gerhard-Domagk-Str. 1, 53121 Bonn, Germany. E-mail: r.streubel@uni-bonn.de; Fax: +49 228 739616; Tel: +49 228 735345*
[b] *Laboratory of Inorganic Chemistry, Department of Chemistry, P.O. Box 55 (A.I. Virtasen aukio 1), FIN-00014 University of Helsinki, Finland*

† Electronic supplementary information (ESI) available: Comparison of the UV/Vis spectrum of complex **9** with calculated vertical singlet excitations of **9** and the cation $\mathbf{9}^+$, as well as calculated molecular orbitals of **9**, $\mathbf{9}^+$, **3b** and **4**. CCDC 767169 (**3a**) and 767316 (**3b**). For ESI and crystallographic data in CIF or other electronic format see DOI: 10.1039/c0nj00151a

‡ This article is part of a themed issue on Main Group chemistry.

HOMO–LUMO gap, through the introduction of a positive charge at the central phosphorus heterocycle.[14,16,22]

We have recently developed a new and facile method for the synthesis of 2*H*-1,4,2-diazaphosphole complexes **III** under mild conditions using 2*H*-azaphosphirene complexes,[26] nitriles and consecutive addition of trifluoromethanesulfonic acid (CF_3SO_3H; hereafter referred to as triflic acid or TfOH) and a base.[27,28] While the substituent in 5-position (R^2) can easily be varied through the choice of the nitrile, so far we only showed that this method can be used for the synthesis of complexes with Ar = Ph, as this substituent is introduced with the 2*H*-azaphosphirene complex. The molecular structures of derivatives of **III** that were determined by single-crystal X-ray diffraction showed in each case an almost perfectly planar phosphorus heterocycle and the remarkable feature of a coplanar arrangement with the 3-phenyl substituent and also—if present—with hetaryl substituents (R^2) at C^5.[27,29] Those complexes showed absorptions at comparatively long wavelengths in their UV/Vis spectra. Furthermore, the protonated intermediates **VI**, observed during the synthesis of **III**, revealed very intense colors.[27] Most of these species turned out to be highly unstable, but when R^2 = NMe_2 they could be isolated. UV/Vis spectra thereof showed remarkable bathochromic shifts for all bands compared to their neutral counter-parts (**III**).[27] It should be noted that acidichroism, *i.e.*, red shift of visual absorption bands upon protonation, has been observed also for some imine derivatives.[30] Furthermore, it has been reported that the emission wavelengths of phosphole-based materials could efficiently be switched by protonation of amino groups that are part of the π-conjugated scaffold.[23]

Against the background of the aforementioned effects of thienyl substituents on the electronic properties of phosphole derivatives **I** and **II**, we decided to synthesize 3-(2-thienyl) substituted 2*H*-1,4,2-diazaphosphole complexes, which are reported in this study. We also present investigations on the photophysical properties of the products and provide an interpretation of the obtained results on the basis of Time-Dependent DFT (TD-DFT) calculations.

Results and discussion

Preparation of 2*H*-1,4,2-diazaphosphole complexes

2*H*-1,4,2-Diazaphosphole complexes **3a,b** were prepared using our newly developed acid/base protocol (Scheme 2). When triflic acid was added to a solution of 2*H*-azaphosphirene complex **1**[31] in the presence of the respective nitrile **2a,b** the initially pale yellow colored reaction mixtures turned immediately

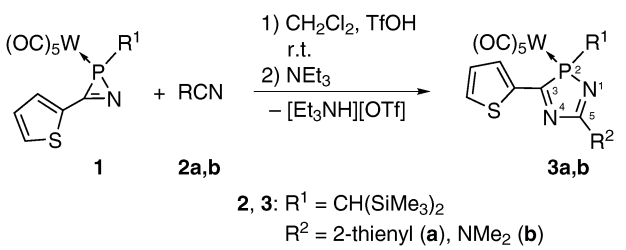

Scheme 2 Synthesis of 2*H*-1,4,2-diazaphosphole complexes **3a,b**.

deep red (**a**) and deep green (**b**), respectively. Upon subsequent addition of triethylamine the solutions turned yellow again and the selective formation of complexes **3a,b** was observed.

Complexes **3a,b** were purified by low-temperature column chromatography and unambiguously characterized by multi-nuclear NMR experiments, mass spectrometry, IR and UV/Vis spectroscopy and single-crystal X-ray diffraction studies (Fig. 1 and 2); their purities were examined by elemental analyses.

The NMR spectra of **3a,b** display characteristic ^{31}P resonances at about 100 ppm with tungsten–phosphorus coupling constant magnitudes of *ca.* 240 Hz. The ^{13}C resonance of the C^3 centers appears at very low field (>195 ppm) and exhibits $|^{2+3}J_{PC}|$ values of about 22 Hz (see Scheme 2 for atom numbering). The C^5 centers resonate at considerably higher field (*ca.* 165 ppm) and have very small phosphorus–carbon coupling constant magnitudes (**3a**: 5.5 Hz; **3b**: 0.6 Hz), thus indicating that at least two scalar couplings contribute to these values. Noteworthy is that the NMe_2 group of **3b** gives rise to two sets of distinctly different ^1H and $^{13}C\{^1H\}$ resonances, which points to a hindered rotation about the C^5–NMe_2 bond.

The C–O stretch vibration bands in the IR spectra of **3a,b** reflect the slightly perturbed C_{4v} symmetry of these complexes. They show each a single, well separated band at around 2070 cm^{-1} and another band with low intensity at *ca.* 1975 cm^{-1}, which can be assigned to normal modes of local A_1 and B_1 symmetry, respectively. In the range of 1900–1950 cm^{-1} two or three very intense and partially overlapping bands appear, which are attributable to vibrations of local A_1 and E symmetry. Two bands according to C–N stretch vibrations were observed at 1540–1600 cm^{-1}.

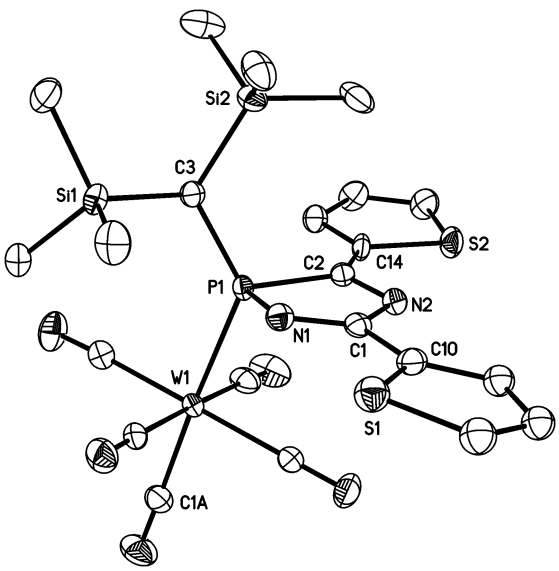

Fig. 1 Molecular structure of complex **3a** in the crystal (hydrogen atoms omitted for clarity; only the prevailing conformation shown, displacement parameters drawn at 50% probability level). Selected bond lengths [Å] and angles [°]: W(1)–P(1) 2.538(1), P(1)–N(1) 1.705(3), P(1)–C(2) 1.858(4), C(2)–N(2) 1.296(5), C(1)–N(1) 1.294(5), C(1)–C(10) 1.445(5), C(2)–C(14) 1.441(5), N(1)–P(1)–C(2) 90.6(2), P(1)–C(2)–N(2) 109.7(2), C(2)–N(2)–C(1) 109.5(3), N(2)–C(1)–N(1) 121.4(3), C(1)–N(1)–P(1) 108.0(2).

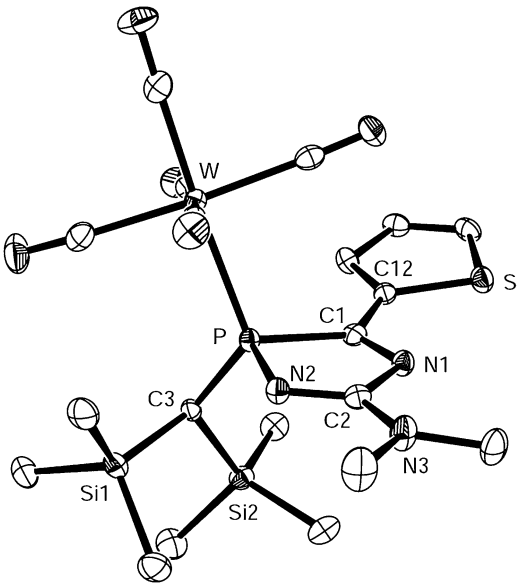

Fig. 2 Molecular structure of complex **3b** in the crystal (hydrogen atoms omitted for clarity, displacement parameters drawn at 50% probability level). Selected bond lengths [Å] and angles [°]: W–P 2.527(1), P–N(2) 1.683(2), P–C(1) 1.879(3), C(1)–N(1) 1.295(4), C(2)–N(2) 1.305(4), C(2)–N(3) 1.343(4), C(1)–C(12) 1.448(4), N(2)–P–C(1) 90.14(13), P–C(1)–N(1) 110.0(2), C(1)–N(1)–C(2) 109.4(3), N(1)–C(2)–N(2) 120.7(3), C(2)–N(2)–P 109.5(2), N(2)–C(2)–N(3) 123.6(3).

In the solid state the molecular structures of both complexes show an essentially planar 2*H*-1,4,2-diazaphosphole ring (mean deviations from least-squares planes: 0.044 (**3a**) and 0.022 Å (**3b**)). It is noteworthy that the three heterocycles in **3a** adopt a largely coplanar arrangement (torsion angles: 6.1° (C2-thienyl–diazaphosphole), 8.5°/9.6° (C1-thienyl–diazaphosphole), and 9.0°/12.4° (C2-thienyl–C1-thienyl)). The thienyl ring at C1 exhibits a statistical disorder (site occupation factors 59 : 41). This feature has also been observed for terminal rings of linear thiophene oligomers.[32] The interring C–C distances between the diazaphosphole and the thienyl substituents are in the range of the lengths for conjugated C_{sp^2}(=N)–CAr bonds (standard value: 1.476(14) Å).[33] Also complex **3b** features a coplanar arrangement of the thienyl ring with respect to the phosphorus heterocycle. The dimethylamino nitrogen atom is almost perfectly trigonal planar coordinated ($\sum_{<}$ 360.5°), and the plane of the NMe_2 group does not deviate significantly from the regression plane of the adjacent heterocycle (deviations from least-squares plane: −0.037 (N3), 0.058 (C10), and −0.080 Å (C11)).

In order to prepare the cationic 2*H*-1,4,2-diazaphospholium complex **4**, the reaction of **1** with dimethyl cyanamide (**2b**) and TfOH was carried out without subsequently adding a base (Scheme 3). The formation of **4** was evidenced by its ^{31}P NMR resonance at δ = 103.3 ($|^{1}J_{WP}|$ = 255.6 Hz) with a phosphorus–proton coupling constant magnitude of 21.6 Hz. However, complex **4** suffered from partial decomplexation during the reaction. The spectrum showed a second resonance at δ = 99.8 ($|^{2+5}J_{PH}|$ = 29.2 Hz) that we assign to the protonated, liberated ligand system **5**, which could not be separated from the former. A similar result was obtained when a pure sample of complex **3b** was reacted with triflic acid.

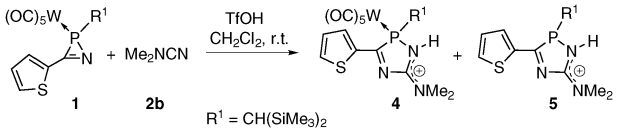

Scheme 3 Attempted synthesis of 2*H*-1,4,2-diazaphospholium complex **4**.

Investigations on the electronic and optical properties of 2*H*-1,4,2-diazaphosphole complexes

The UV/Vis absorption spectra of complexes **3a,b** show a strong band at λ_{max} = 341 (lg ε = 4.28; **3a**) and 325 nm (lg ε = 4.19; **3b**), respectively, and another band at very long wavelength but with low intensity (**3a**: λ_{max} = 444 nm, lg ε = 3.41; **3b**: λ_{max} = 413 nm, lg ε = 3.54). Compared to analogous 3-phenyl substituted 2*H*-1,4,2-diazaphosphole complexes,[27,29] these bands are bathochromic shifted by 4–24 nm. The lowest-energy absorptions are at even longer wavelengths than the π–π* transitions of phosphole complex derivatives **6**[14] and **7**[24] (Scheme 4). Noteworthy are also the long-wave optical end absorptions (λ_{onset}) of **3a** (584 nm) and **3b** (525 nm). For comparison, for complex **6** a value of 475 nm was reported.[14]

The largely coplanar arrangement in the crystal state of the three adjacent ring systems in **3a** as well as the two ring systems and the dimethylamino group in **3b** may allow for extended π conjugation. Since the 2*H*-1,4,2-diazaphosphole ring can be devised from the phosphole ring by replacement of two CR units by nitrogen atoms, an even lower LUMO energy may be expected for 2*H*-1,4,2-diazaphosphole complexes compared to complexes of phospholes. This was evidenced from cyclovoltammetric investigations, which revealed that complex **3a** is reversibly reduced at $E_{1/2}$ = −1.635 V (calc. *vs.* $E_{1/2}(FeCp_2^{+}/FeCp_2)$) (Fig. 3A). Complex **6** showed an irreversible reduction wave at more negative potential under comparable conditions (E_{pc} = −2.20 V).[14] On the other hand, phosphole complex **6** exhibited a slightly lower anodic peak potential (E_{pa} = +0.70 V)[14] than **3a** (E_{pa} = +0.83 V; Fig. 3B), which points to a higher HOMO energy in the former case; for both complexes the electrochemical oxidations were irreversible under the applied measuring conditions.

In order to provide an interpretation of the UV/Vis absorption bands of 2*H*-1,4,2-diazaphosphole complexes, vertical singlet excitations were calculated for the di(2-thienyl) substituted derivative **3a** by means of Time-Dependent Density Functional

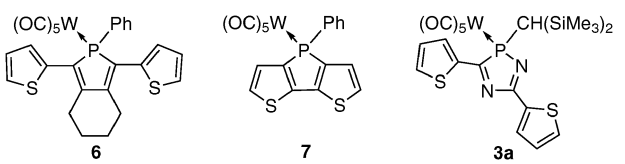

Scheme 4 Comparison of the long-wave absorption maxima for complexes **3a**, **6** and **7**.

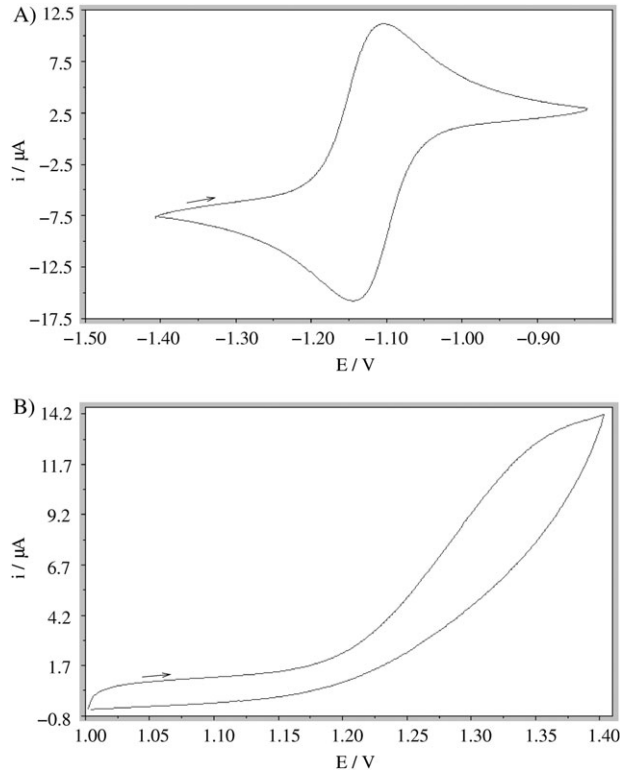

Fig. 3 Cyclic voltammogram of **3a** in CH_2Cl_2 (3 mM; 0.1 M [^{n}Bu$_4$N][PF$_6$]) (A) between −1.40 and −0.82 V and (B) between +1.00 and +1.40 V *vs.* Ag/AgCl/2 M LiCl in EtOH (GCE, Pt-wire; scan rate 0.1 V s^{-1}; T = 25 °C).

Theory (TD-DFT).[34] In Fig. 4 the computed data are plotted in comparison to the experimentally recorded UV/Vis spectrum in wavenumbers.§

All relevant electronic transitions (Table 1) occur into the **LUMO** (Fig. 5). This is unambiguously characterized as a π* orbital of the heterocyclic system extended over all three rings, whereas by far the largest contribution is given by the carbon and nitrogen atoms of the diazaphosphole ring. As the contribution of phosphorus is negligible, a σ*–π* hyperconjugation, *i.e.*, the interaction of a σ* orbital of the exocyclic bonds at P with a virtual orbital of the adjacent π-system, as discussed for phosphole derivatives[15,18] and similarly for silole, germole and stannole derivatives,[8] is not supported here. The first excitation of considerable oscillator strength is predicted at 19 870 cm^{-1} (No. 2) occurring from the **HOMO** − **1**. Because the latter shows clearly the characteristics of a metal d orbital, this transition is described as a metal–ligand charge transfer (MLCT) process. Against the background that the applied calculation method yields excitation energies that might by trend be somewhat too low,[35] an assignment of the weak low-energy band detected at 22 500 cm^{-1} (λ = 444 nm) to this MLCT process is plausible.

The more intense absorption band centered at 29 400 cm^{-1} (λ_{max} = 341 nm) might arise from superposition of excitation No. 4 and two further nearly degenerate excitations, No. 6 and 8. In the former the electron is excited from **HOMO** − **3**, which is an almost pure π orbital wherein the dominance of the thienyl ring at C^5 is clearly evident. Therefore, this excitation can be assigned to a π–π* transition with an intramolecular charge transfer character from the thienyl group at C^5 to the diazaphosphole ring. The excitations No. 6 and 8 both occur from **HOMO** − **4** and **HOMO** − **6** into the **LUMO**. While the **HOMO** − **4** exhibits distinct π characteristics and is uniformly distributed over all three heterocycles, the **HOMO** − **6** (not shown) has mainly σ character and the largest amplitude is found at the nitrogen lone pairs. Consequently, the corresponding excitations may be described as mixtures of π–π* and n–π* transitions.

As the 3-(2-thienyl) substituted cationic complex **4** could not be isolated, the effect of *N*-protonation on the photophysical properties of 2*H*-1,4,2-diazaphosphole complexes is discussed on the example of the 3-phenyl derivatives[27] **8** and **9** (Fig. 6). An inspection of their UV/Vis spectra reveals that the longest-wavelength absorption maximum of **9** is significantly bathochromic shifted with respect to that of the neutral complex **8** ($\Delta\nu_{max} \approx 3000$ cm^{-1}). This band has a very broad shape and the long tail in the visible region is giving rise to an extremely long-wave optical end absorption (λ_{onset} = 649 nm; ν_{onset} = 15 400 cm^{-1}). Another remarkable effect of protonation is a pronounced increase in the molar absorptivity of the band in the region of the π–π* transitions (**8**: ν_{max} = 34 700 cm^{-1}, lg ε = 4.24; **9**: ν_{max} = 32 700 cm^{-1}, lg ε = 4.45).

We carried out TD-DFT calculations on the neutral complex **8** (Table 2A) and the *N*-protonated complex **9** (Table 2B), the latter with TfO$^-$ attached *via* an N–H–O hydrogen bond.¶ The molecular orbitals of **8** and **9** can be classified as either being of π type or constituting a metal d orbital or a lone pair at nitrogen (n). For most MOs of **9** congeners to the orbitals of **8** (Fig. 7) can be found (see ESI†). Because some have a different energetical order, they were labeled for both complexes as π_i, d_i or n in order to facilitate the comparison.

The major effects caused by protonation of **8** can be summarized as follows. All orbital energies are significantly decreased but to a different extent (Table 3). Protonation at the diazaphosphole ring has a stronger impact on the orbitals being localized at this ring than on metal-centered orbitals. For example, the energy of the **LUMO**, which is a π orbital (π*) with the largest contribution at the phosphorus heterocycle, is lowered by 0.9 eV. As the effect on d_1 and d_2 is significantly lower ($\Delta\varepsilon(d_1)$ = 0.51 eV and $\Delta\varepsilon(d_2)$ = 0.45 eV), the excitation energies for the MLCT processes $d_1 \rightarrow \pi^*$ and $d_2 \rightarrow \pi^*$ are decreased. These effects explain the observed bathochromic shift of the longest-wavelength band and the resulting pronounced long-wave optical end absorption of the protonated complex.

The π_3 orbital, which is localized at the amidine moiety, is even more effected through the perturbation induced by protonation than the **LUMO**; its energy is decreased by even 1.21 eV. Consequently, the corresponding excitation is blue

§ Data are given in wavenumbers because of the direct proportionality to excitation energies. In the tables the calculated transitions are numbered according to increasing wavenumbers.

¶ When the counterion was omitted (using the cationic model system **9**$^+$) the excitation energies obtained were in poorer agreement with the experimental results (see ESI†).

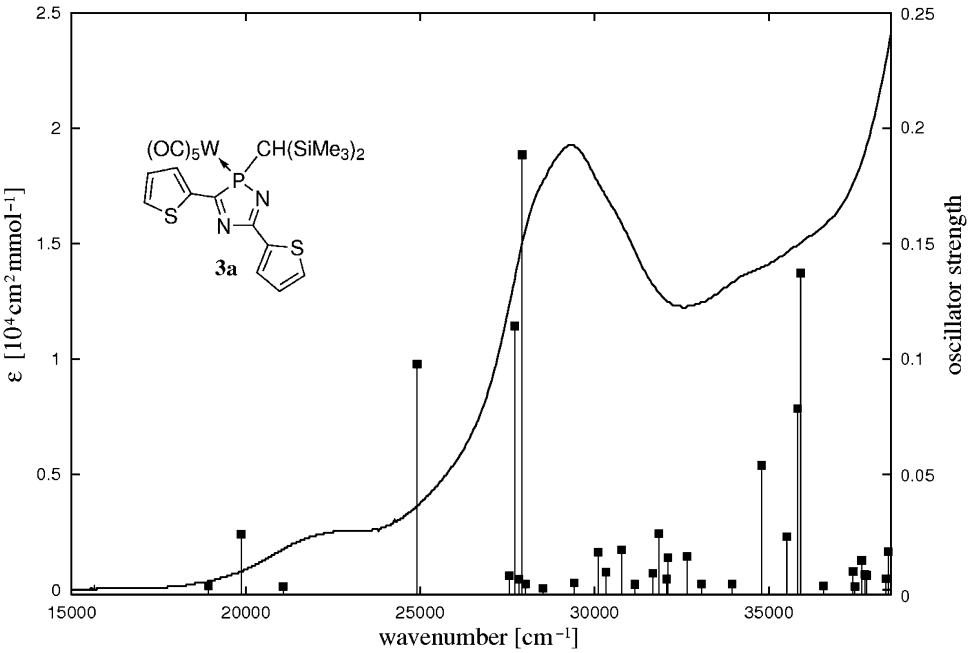

Fig. 4 UV/Vis spectrum (continuous spectrum, solid line; *n*-pentane) and calculated vertical singlet excitations for **3a** (line spectrum; TD-B3LYP/SV(P)/ECP-60-MWB(W)//RI-BLYP/SV(P)/ECP-60-MWB(W)).

Table 1 Selected vertical singlet excitations calculated for complex **3a** (only the major orbital contributions given)

No.	ν/ cm^{-1}	Oscillator strength	Orbital contributions	$\|c\|^2$ (%)
2	19 870	0.024	**HOMO − 1 → LUMO**	98
4	24 912	0.098	**HOMO − 3 → LUMO**	88
6	27 721	0.114	**HOMO − 6 → LUMO**	47
			HOMO − 4 → LUMO	35
8	27 928	0.189	**HOMO − 4 → LUMO**	51
			HOMO − 6 → LUMO	24

shifted (*cf.* No. 4 of complex **8** and No. 5 of complex **9**). However, the strongest absorption maximum in the spectra of **8** and **9** arises from the superposition of three (complex **8**: No. 15, 17 and 19) or two (complex **9**: No. 14 and 16) nearly degenerate excitations. The π orbitals that are involved in these transitions are clearly polarized towards (π_2) or largely restricted to the phenyl substituent (π_1) and are therefore somewhat less affected through protonation than the **LUMO**.‖ As a consequence, the corresponding transitions are bathochromic shifted, which is consistent with the experimental results.

In order to provide a projection for the anticipated properties of the 3-(2-thienyl) substituted protonated complex **4**, vertical singlet excitations were additionally calculated for this derivative (Table 4 and ESI†). Qualitatively, this yielded a similar picture as for **9**. However, all calculated transitions of **4** appear at even longer wavelengths.

Conclusions

The synthesis of 3-(2-thienyl) substituted 2*H*-1,4,2-diazaphosphole complexes **3a,b** with our newly developed acid/base protocol was presented. Their molecular structures show ligands that possess a completely coplanar arrangement of the diazaphosphole rings with both thienyl groups (**3a**) and with the thienyl and the NMe_2 group (**3b**), which allows extended π conjugation over the planar framework. As a result, complexes **3a,b** exhibit interesting photophysical properties. Compared to their 3-phenyl substituted analogs, all UV/Vis absorption bands of **3a,b** are bathochromic shifted. They show one transition at very long wavelength, which is assigned to a metal–ligand charge transfer (MLCT) process, and one strong band close to the wavelength range of the π–π* excitations of π-conjugated phosphole complexes. This band results from a superposition of π–π* and n–π* transitions. Upon *N*-protonation of the 2*H*-1,4,2-diazaphosphole ring the intensity of the latter excitation significantly increases and all bands experience a pronounced red shift, resulting in a very long-wavelength optical end absorption. These effects can be explained by the different extent to which the orbital energies are influenced through protonation. Metal d orbitals are significantly less affected than the π-orbitals with a large contribution near the protonated site.

Currently, we are investigating the possibility to modify the phosphorus center of 2*H*-1,4,2-diazaphosphole complexes *via* decomplexation and/or oxidation, which may lead to different interesting electronic and optical properties of this heterocycle. Furthermore, the ease with which thienyl groups can be

‖ In the case of complex **8** the **HOMO − 7** (n) shows a large contribution to excitations No. 17 and 19. This orbital corresponds to the lone pair at N^1, hence, an analog is missing in **9** as this lone pair is protonated. On the other hand, complex **9** exhibits two orbitals, **HOMO − 7** and **HOMO − 10**, that have no congener in complex **8**. They are mainly localized at the oxygen atoms of triflate and contribute, together with π_1 and π_2, to the very intense excitation No. 16. Therefore, this excitation is not described as a pure π–π* transition as it additionally has certain characteristics of an anion–cation charge transfer process.

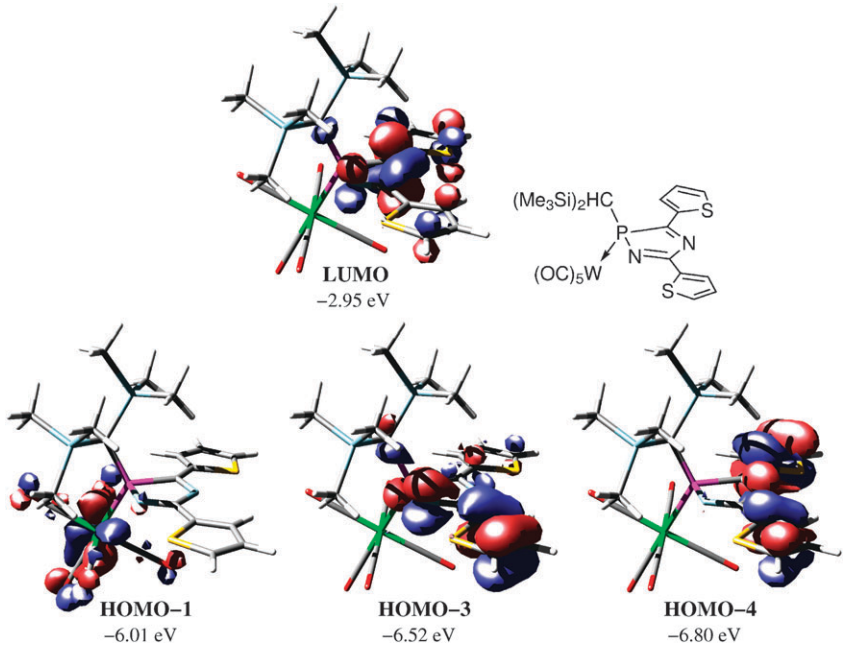

Fig. 5 Visualization of selected molecular orbitals calculated for **3a** (B3LYP/SV(P)/ECP-60-MWB(W); isovalue 0.04 au).

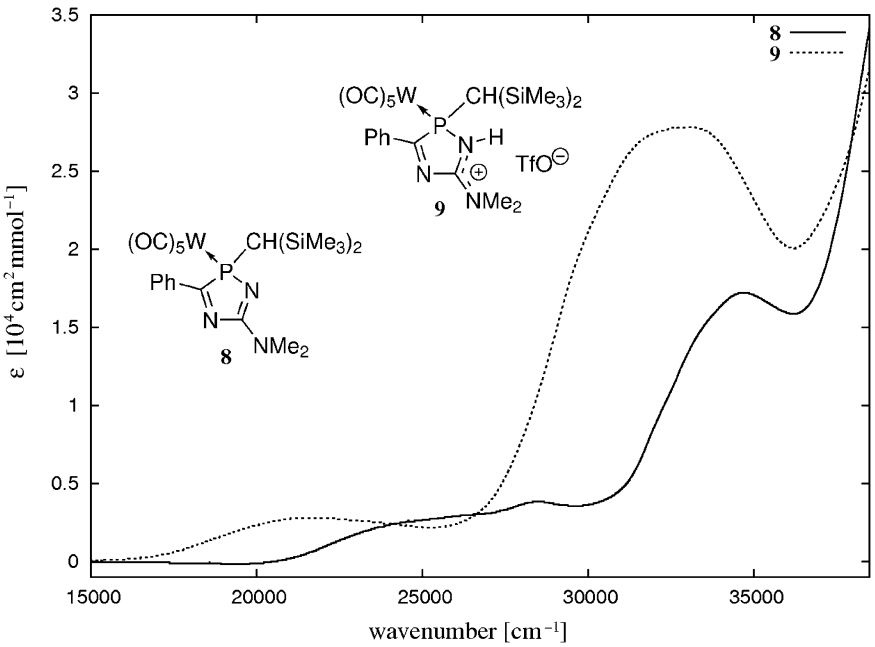

Fig. 6 UV/Vis spectra of complexes **8** (solid line; *n*-pentane) and **9** (dashed line; CH_2Cl_2).

functionalized may now allow the preparation of larger π-conjugated oligomeric or polymeric systems.

Experimental

General procedures

All manipulations were carried out in an atmosphere of purified and dried argon using standard Schlenk techniques. Solvents were dried over sodium wire or CaH_2 (CH_2Cl_2) and distilled under argon. 2*H*-Azaphosphirene complex **1**[31] was prepared according to the method described in the literature. Triflic acid, dimethyl cyanamide and 2-thiophenecarbonitrile were purchased from Acros. Melting points were determined using a Büchi apparatus type S; the values are not corrected. Elemental analyses were performed by using an Elementar VarioEL instrument. UV/Vis absorption spectra were recorded on a Shimadzu UV-1650 PC spectrometer (λ = 190–1100 nm) from *n*-pentane solution at ambient temperature and IR spectra were recorded as KBr pellets using a Thermo Nicolet 380 FT-IR spectrometer. NMR data were recorded on a Bruker Avance 300 spectrometer at 30 °C using C_6D_6 as solvent and internal standard; coupling constants *J* are

Table 2 Selected vertical singlet excitations calculated for complexes **8** and **9** (only the major orbital contributions given)

No.	ν/cm^{-1}	Oscillator strength	Orbital contributions[a]	$\|c\|^2$ (%)
(A)			Complex **8**	
1	20 912	0.003	**HOMO** (d_2) → **LUMO** (π^*)	99
2	21 867	0.020	**HOMO** − **1** (d_1) → **LUMO** (π^*)	99
4	25 183	0.046	**HOMO** − **3** (π_3) → **LUMO** (π^*)	85
15	32 992	0.111	**HOMO** − **4** (π_2) → **LUMO** (π^*)	42
			HOMO − **6** (π_1) → **LUMO** (π^*)	28
17	33 636	0.085	**HOMO** − **7** (n) → **LUMO** (π^*)	44
			HOMO − **4** (π_2) → **LUMO** (π^*)	19
19	33 898	0.137	**HOMO** − **7** (n) → **LUMO** (π^*)	35
			HOMO − **4** (π_2) → **LUMO** (π^*)	29
(B)			Complex **9**	
1	17 355	0.010	**HOMO** (d_2) → **LUMO** (π^*)	93
2	18 730	0.021	**HOMO** − **1** (d_1) → **LUMO** (π^*)	90
5	26 731	0.013	**HOMO** − **4** (π_3) → **LUMO** (π^*)	81
14	30 950	0.060	**HOMO** − **9** (π_1) → **LUMO** (π^*)	69
			HOMO − **6** (π_2) → **LUMO** (π^*)	25
16	32 072	0.209	**HOMO** − **7** → **LUMO** (π^*)	37
			HOMO − **6** (π_2) → **LUMO** (π^*)	23
			HOMO − **9** (π_1) → **LUMO** (π^*)	18
			HOMO − **10** → **LUMO** (π^*)	12

[a] See Fig. 7 for orbital denotation.

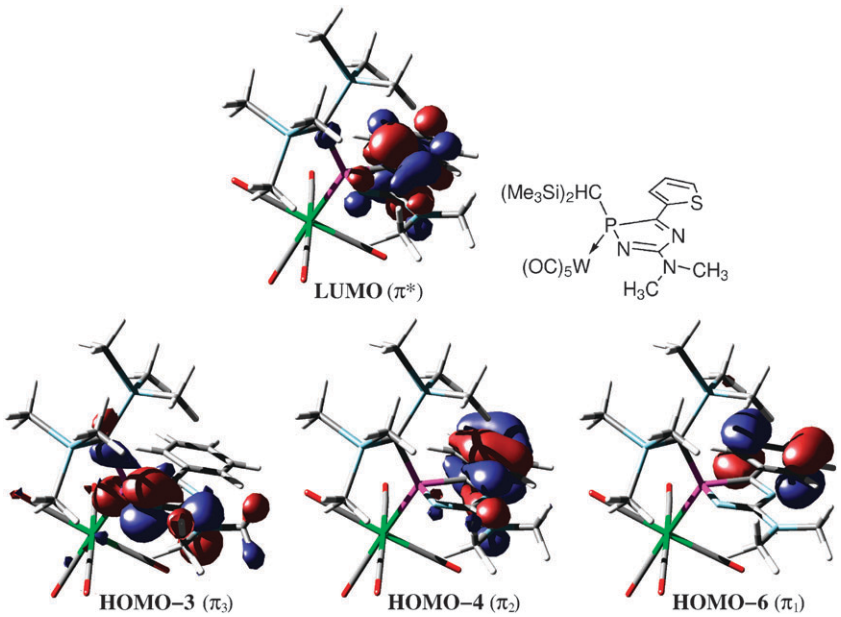

Fig. 7 Visualization of selected molecular orbitals calculated for **8** (B3LYP/SV(P)/ECP-60-MWB(W); isovalue 0.04 au).

Table 3 Calculated orbital energies ε [eV] for complexes **8** and **9**

Orbital[a]	Orbital energies of complex **8**	Orbital energies of complex **9**
π^*	−2.55 (**LUMO**)	−3.45 (**LUMO**)
d_2	−5.81 (**HOMO**)	−6.26 (**HOMO**)
d_1	−5.87 (**HOMO** − **1**)	−6.38 (**HOMO** − **1**)
π_3	−6.30 (**HOMO** − **3**)	−7.51 (**HOMO** − **4**)
π_2	−7.09 (**HOMO** − **4**)	−7.75 (**HOMO** − **6**)
π_1	−7.33 (**HOMO** − **6**)	−7.94 (**HOMO** − **9**)
n	−7.64 (**HOMO** − **7**)	—

[a] See Fig. 7 for orbital denotation.

reported in Hz, chemical shifts in ppm relative to tetramethylsilane (^{1}H: 300.13, ^{13}C: 75.5, ^{29}Si: 59.6 MHz) and 85% H_3PO_4 (^{31}P: 121.5 MHz). Mass spectra were recorded on a Kratos Concept 1H (FAB+, *m*NBA) spectrometer (selected data given). Cyclovoltammetric measurements (CV) were performed using an EG&G-Potentiostat/Galvanostat M273 in CH_2Cl_2 with 0.1 M [*n*-Bu_4N][PF_6] as supporting electrolyte at a glassy carbon electrode (GCE) with an Ag/AgCl/2M LiCl reference electrode (Pt-wire as counter electrode; scan rate 0.1 V s^{-1}; T = 25 °C).

Preparation of 2*H*-1,4,2-diazaphosphole complexes

[2-Bis(trimethylsilyl)methyl-3,5-di(2-thienyl)-2*H*-1,4,2-diazaphosphole-κ*P*]pentacarbonyltungsten(0) (3a). To a stirred solution of 2*H*-azaphosphirene complex **1** (250 mg, 0.40 mmol) in CH_2Cl_2 (5.5 cm^3) were added consecutively

Table 4 Selected vertical singlet excitations calculated for complex **4** (only the major orbital contributions given)

No.	ν/cm^{-1}	Oscillator strength	Orbital contributions	$\|c\|^2$ (%)
1	17 041	0.010	**HOMO** (d_2) → **LUMO** (π^*)	93
2	18 291	0.018	**HOMO** − **1** (d_1) → **LUMO** (π^*)	91
5	26 434	0.021	**HOMO** − **5** (π_3) → **LUMO** (π^*)	54
			HOMO − **4** (π_2) → **LUMO** (π^*)	32
11	29 232	0.249	**HOMO** − **4** (π_2) → **LUMO** (π^*)	56
			HOMO − **8** → **LUMO** (π^*)	18
			HOMO − **5** (π_3) → **LUMO** (π^*)	15

2-thiophenecarbonitrile (40 mm^3, 0.42 mmol) and triflic acid (37 mm^3, 0.42 mmol) at ambient temperature. The initially yellow colored solution turned deep green. Subsequently, NEt_3 (58 mm^3, 0.41 mmol) was added at ambient temperature while the reaction mixture turned brownish yellow. Then all volatiles were removed *in vacuo* (~1 Pa) and the product was purified by column chromatography on silica (−20 °C, 2 × 8 cm) using petroleum ether/Et_2O (100 : 1) as eluent. Evaporation of the solvents of the first fraction (~1 Pa) yielded complex **3a** (193 mg, 0.26 mmol, 66%) as an orange solid; mp 128 °C (found: C, 35.8; H, 3.4; N, 4.2; S, 8.6%. Calc. for $C_{22}H_{25}N_2O_5PS_2Si_2W$: C, 36.1; H, 3.4; N, 3.8; S, 8.8%); λ_{max}/nm 444 (ε/dm^3 mol^{-1} cm^{-1} 2557), 341 (19 260), 287sh (13 985), 249sh (38 120), 232 (59 618); ν_{max}/cm^{-1} 2963w and 2904w (CH_3/CH), 2069m, 1977m, 1935s and 1925s (CO), 1557m and 1545m (CN), 1261m (thienyl); δ_H −0.18 (9H, s_{sat}, J_{CH} 119.7, $SiMe_3$), 0.53 (9H, s_{sat}, J_{CH} 120.1, $SiMe_3$), 1.09 (1H, d, J_{PH} 3.7, C*H*($SiMe_3$)$_2$), 6.63 (1H, dd, J_{HH} 4.8 and 3.9, thienyl-C(4)H at diazaphosphole-C(5)), 6.74 (1H, dd, J_{HH} 5.0 and 3.9, thienyl-C(4)H at diazaphosphole-C(3)), 6.88 (1H, dd, J_{HH} 4.8 and 1.1, thienyl-C(5)H at diazaphosphole-C(5)), 6.89 (1H, ddd, J_{PH} 1.2, J_{HH} 5.0 and 1.1, thienyl-C(5)H at diazaphosphole-C(3)), 7.86 (1H, dd, J_{HH} 3.9 and 1.1, thienyl-C(3)H at diazaphosphole-C(3)), 8.05 (1H, dd, J_{HH} 3.9 and 1.1, thienyl-C(3)H at diazaphosphole-C(5)); δ_C 2.7 (d_{sat}, J_{PC} 2.3, J_{SiC} 52.5, $SiMe_3$), 3.7 (d_{sat}, J_{PC} 2.9, J_{SiC} 53.4, $SiMe_3$), 20.0 (d, J_{PC} 4.8, *C*H($SiMe_3$)$_2$), 128.6 (s, thienyl-C(4) at diazaphosphole-C(3)), 128.6 (d, J_{PC} 0.9, thienyl-C(4) at diazaphosphole-C(5)), 133.4 (s, thienyl-C(5) at diazaphosphole-C(5)), 134.2 (d, J_{PC} 0.9, thienyl-C(3) at diazaphosphole-C(5)), 134.7 (s, thienyl-C(5) at diazaphosphole-C(3)), 137.8 (s, thienyl-C(3) at diazaphosphole-C(3)), 137.8 (d, J_{PC} 27.8, thienyl-C(2) at diazaphosphole-C(3)), 138.5 (d, J_{PC} 14.5, thienyl-C(2) at diazaphosphole-C(5)), 165.5 (d, J_{PC} 5.5, PNC), 195.2 (d_{sat}, J_{WC} 3.6, J_{PC} 22.3, PCN), 197.6 (d_{sat}, J_{WC} 126.7, J_{PC} 6.1, CO_{cis}), 198.4 (d_{sat}, J_{WC} 143.5, J_{PC} 22.6, CO_{trans}); δ_{Si} 3.5 (d_{sat}, J_{PSi} 11.8, J_{SiC} 52.5), 3.5 (d_{sat}, J_{PSi} 2.5, J_{SiC} 53.4); δ_P 110.4 (d_{sat}, J_{WP} 235.2, J_{PH} 3.3); *m*/*z* 733 ([M + H]$^+$, 11%), 704 (M$^+$ − CO, 17), 676 (M$^+$ − 2CO, 34), 648 (M$^+$ − 3CO, 49), 592 (M$^+$ − 5CO, 13), 509 ([M + H]$^+$ − $W(CO)_5$, 100).

[2-Bis(trimethylsilyl)methyl-5-dimethylamino-3-(2-thienyl)-2*H*-1,4,2-diazaphosphole-κ*P*]pentacarbonyltungsten(0) (3b). To a stirred solution of 2*H*-azaphosphirene complex **1** (310 mg, 0.50 mmol) in CH_2Cl_2 (6.2 cm^3) were added consecutively dimethyl cyanamide (42 mm^3, 0.52 mmol) and triflic acid (42 mm^3, 0.48 mmol) at ambient temperature. The initially yellow colored solution turned deep red. Subsequently, NEt_3 (68 mm^3, 0.48 mmol) was added at ambient temperature while the reaction mixture turned yellow again. After removal of all volatiles *in vacuo* (~1 Pa) the crude product was dissolved in petroleum ether, filtered through Celite, and purified by column chromatography on silica (−35 °C, 2 × 10 cm) using petroleum ether/Et_2O (100 : 1) as eluent. Evaporation of the solvents of the first fraction (~1 Pa) yielded complex **3b** (246 mg, 0.35 mmol, 71%) as an orange solid; mp 133 °C (found: C, 34.7; H, 4.1; N, 6.2; S, 4.8%. Calc. for $C_{20}H_{28}N_3O_5PSSi_2W$: C, 34.6; H, 4.1; N, 6.1; S, 4.6%); λ_{max}/nm 413sh (ε/dm^3 mol^{-1} cm^{-1} 3459), 325 (15 341), 292sh (10 678), 250sh (41 259), 232 (72 442), 212sh (43 465); ν_{max}/cm^{-1} 2962w, 2930w, 2901w and 2878w (CH_3/CH), 2066m, 1976m, 1942s, 1929s and 1906s (CO), 1604m and 1540w (CN), 1262m and 1251m (thienyl); δ_H −0.14 (9H, s_{sat}, J_{CH} 119.4, $SiMe_3$), 0.51 (9H, s_{sat}, J_{CH} 119.5, $SiMe_3$), 1.04 (1H, d, J_{PH} 3.3, C*H*($SiMe_3$)$_2$), 2.80 (3H, s, NMe), 2.92 (3H, s, NMe), 6.78 (1H, dd, J_{HH} 5.0 and 3.9, thienyl-C(4)H), 6.95 (1H, d, J_{HH} 5.0, thienyl-C(5)H), 7.87 (1H, d, J_{HH} 3.9, thienyl-C(3)H); δ_C 3.0 (d_{sat}, J_{PC} 1.6, J_{SiC} 52.7, $SiMe_3$), 4.0 (d_{sat}, J_{PC} 2.6, J_{SiC} 52.7, $SiMe_3$), 23.2 (d, J_{PC} 5.8, *C*H($SiMe_3$)$_2$), 37.6 (s, NMe), 37.7 (s, NMe), 128.4 (s, thienyl-C(4)), 133.7 (s, thienyl-C(5)), 137.2 (s, thienyl-C(3)), 137.9 (d, J_{PC} 25.2, thienyl-C(2)), 165.1 (d, J_{PC} 0.6, PNC), 193.3 (d_{sat}, J_{WC} 3.6, J_{PC} 25.2, PCN), 198.5 (d_{sat}, J_{WC} 126.7, J_{PC} 6.8, CO_{cis}), 199.7 (d_{sat}, J_{WC} 142.9, J_{PC} 22.3, CO_{trans}); δ_{Si} 1.7 (d_{sat}, J_{PSi} 12.0, J_{SiC} 52.7), 2.1 (d_{sat}, J_{PSi} 2.5, J_{SiC} 52.7); δ_P 104.0 (d_{sat}, J_{WP} 245.4, J_{PH} 2.2); *m*/*z* 694 ([M + H]$^+$, 7%), 665 (M$^+$ − CO, 29), 637 (M$^+$ − 2CO, 27), 581 (M$^+$ − 4CO, 29), 370 ([M + H]$^+$ − $W(CO)_5$, 100).

X-Ray crystallography

X-Ray crystallographic analyses of 3a,b. Suitable orange single crystals of **3a** and yellow single crystals of **3b** were obtained from concentrated *n*-pentane solutions upon decreasing the temperature from ambient temperature to +4 °C. Data were collected on a Nonius KappaCCD diffractometer equipped with a low-temperature device (Cryostream, Oxford Cryosystems) at 123 (**3a**) or 100 K (**3b**) using graphite monochromated Mo-Kα radiation (λ = 0.71073 Å). The structures were solved by Direct Methods (**3a**) or Patterson methods (**3b**) (SHELXS-97)[36] and refined by full-matrix least squares on F^2 (SHELXL-97).[36] All non-hydrogens were refined anisotropically. The hydrogen atoms were included isotropically using the riding model on the bound atoms. Absorption corrections were carried out analytically (**3b**) or semi-empirically from equivalents (**3a**) (min./max. transmissions = 0.36309/0.53875 (**3a**) and 0.3949/0.8787 (**3b**)). In **3a** the thienyl group at C1 is disordered. The disordered atoms were refined isotropically with constraint for the displacement parameters

and restraints for bond distances and angles. For more information see the cif-file.†

Crystal structure data for complex 3a ($C_{22}H_{25}N_2O_5PS_2Si_2W$). Crystal size 0.35 × 0.20 × 0.15 mm, triclinic, $P\bar{1}$ (No. 2), a = 9.5035(3), b = 10.9580(4), c = 15.4221(7) Å, α = 75.868(2)°, β = 84.937(2)°, γ = 65.551(2)°, V = 1417.64(9) Å^3, Z = 2, ρ_{calc} = 1.716 Mg m^{-3}, $2\theta_{max}$ = 55°, collected (independent) reflections = 13 970 (6484), R_{int} = 0.0401, μ = 4.397 mm^{-1}, 309 refined parameters, 119 restraints, R_1 (for $I > 2\sigma(I)$) = 0.0291, wR_2 (for all data) = 0.0686, S = 1.040, max./min. residual electron density = 1.268/−2.092 e Å^{-3}.

Crystal structure data for complex 3b ($C_{20}H_{28}N_3O_5PSSi_2W$). Crystal size 0.26 × 0.20 × 0.03 mm, monoclinic, $P2_1/n$, a = 11.8239(2), b = 20.2887(5), c = 11.9270(3) Å, β = 104.5180(10)°, V = 2769.83(11) Å^3, Z = 4, ρ_{calc} = 1.663 Mg m^{-3}, $2\theta_{max}$ = 55°, collected (independent) reflections = 44 556 (6333), R_{int} = 0.0569, μ = 4.423 mm^{-1}, 306 refined parameters, 0 restraints, R_1 (for $I > 2\sigma(I)$) = 0.0290, wR_2 (for all data) = 0.0541, S = 0.983, max./min. residual electron density = 2.001/−1.875 e Å^{-3}.

Computational methods

DFT calculations were carried out with the TURBOMOLE V5.9.1 program package.[37] The structures were optimized[38] with the gradient corrected exchange functional by Becke[39] (B88) in combination with the gradient corrected correlation functional by Lee and coworkers[40] (LYP) with the RI approximation[41] and the valence-double-ζ basis set SV(P).[42] The core electrons of tungsten were substituted by the effective core potential ECP-60-MWB.[43] All stationary points were characterized as minima by analytical vibrational frequency calculations.[44] Vertical singlet excitations were calculated by means of Time-Dependent Density Functional Theory (TD-DFT)[34] using the Three Parameter Hybrid Functional Becke3 (B3)[45] in combination with the LYP functional,[40] the SV(P)[42] basis set and ECP-60-MWB[43] for tungsten.

Acknowledgements

Financial support by the DFG (STR 411/25-2), the COST action CM0802 "PhoSciNet" and the Fonds der Chemischen Industrie (Kekulé grant for H. Helten) is gratefully acknowledged.

Notes and references

1 *Electronic Materials: The Oligomer Approach*, ed. K. Müllen and G. Wegner, Wiley-VCH, Weinheim, 1998; *Handbook of Conducting Polymers*, ed. T. A. Skotheim, R. L. Elsenbaumer, and J. R. Reynolds, Marcel Dekker, New York, 1998; A. Kraft, A. C. Grimsdale and A. B. Holmes, *Angew. Chem.*, 1998, **110**, 416–443 (*Angew. Chem., Int. Ed.*, 1998, **37**, 403–428); P. F. H. Schwab, J. R. Smith and J. Michl, *Chem. Rev.*, 2005, **105**, 1197–1279; F. J. M. Hoeben, P. Jonkheijm, E. W. Meijer and A. P. H. J. Schenning, *Chem. Rev.*, 2005, **105**, 1491–1546.
2 *Organic Light Emitting Devices*, ed. K. Müllen and U. Scherf, Wiley-VCH, Weinheim, 2005.
3 H. E. Katz and Z. Bao, *J. Phys. Chem. B*, 2000, **104**, 671–678.
4 G. A. Chamberlain, *Sol. Cells*, 1983, **8**, 47–83.
5 D. T. McQuade, A. E. Pullen and T. M. Swager, *Chem. Rev.*, 2000, **100**, 2537–2574.
6 J. Roncali, *Chem. Rev.*, 1997, **97**, 173–205; F. Garnier, *Acc. Chem. Res.*, 1998, **32**, 209–215; R. E. Martin and F. Diederich, *Angew. Chem.*, 1999, **111**, 1440–1469 (*Angew. Chem., Int. Ed.*, 1999, **38**, 1350–1377); J. M. Tour, *Acc. Chem. Res.*, 2000, **33**, 791–804; U. Mitschke and P. Bäuerle, *J. Mater. Chem.*, 2000, **10**, 1471–1507; J. L. Segura and N. Martin, *J. Mater. Chem.*, 2000, **10**, 2403–2435; F. Fichou, *J. Mater. Chem.*, 2000, **10**, 571–588; T.-Q. Nguyen, J. Wu, V. Doan, B. J. Schwartz and S. H. Tolbert, *Science*, 2000, **288**, 652–656; M. A. Baldo, M. E. Thompson and S. R. Forrest, *Nature*, 2000, **403**, 750–752; Y. Shi, C. Zhang, H. Zhang, J. H. Bechtel, L. R. Dalton, B. H. Robinson and W. H. Steier, *Science*, 2000, **288**, 119–122.
7 Z. Zhou, T. Maruyama, T. Kanbara, T. Ikeda, K. Ichimura, T. Yamamoto and K. Tokuda, *J. Chem. Soc., Chem. Commun.*, 1991, 1210–1212; T. Yamamoto, Z.-H. Zhou, T. Kanbara, M. Shimura, K. Kizu, T. Maruyama, Y. Nakamura, T. Fukuda, B. L. Lee, N. Ooba, S. Tomura, T. Kurihara, T. Kaino, K. Kubota and S. Sasaki, *J. Am. Chem. Soc.*, 1996, **118**, 10389–10399; Q. T. Zhang and J. T. Tour, *J. Am. Chem. Soc.*, 1998, **120**, 5355–5362; D. J. Irvin, C. J. Dubois and J. R. Reynolds, *Chem. Commun.*, 1999, 2121–2122.
8 S. Yamaguchi, Y. Itami and K. Tamao, *Organometallics*, 1998, **17**, 4910–4916.
9 K. Tamao, S. Yamaguchi, M. Shiozaki, Y. Nakagawaa and Y. Ito, *J. Am. Chem. Soc.*, 1992, **114**, 5867–5869; K. Tamao, M. Uchida, T. Izumizawa, K. Furukawa and S. Yamaguchi, *J. Am. Chem. Soc.*, 1996, **118**, 11974–11975; S. Yamaguchi, Y. Itami and K. Tamao, *Organometallics*, 1998, **17**, 4910–4916; S. Yamaguchi and K. Tamao, *J. Chem. Soc., Dalton Trans.*, 1998, 3693–3702; S. Yamaguchi, T. Goto and K. Tamao, *Angew. Chem.*, 2000, **112**, 1761–1763 (*Angew. Chem., Int. Ed.*, 2000, **39**, 1695–1697); S. Yamaguchi, T. Endo, M. Uchida, T. Izumizawa, K. Furukawa and K. Tamao, *Chem.–Eur. J.*, 2000, **6**, 1683–1692.
10 The first polymer containing phosphole rings in the backbone was reported by Tilley and coworkers: S. S. H. Mao and T. D. Tilley, *Macromolecules*, 1997, **30**, 5566–5569.
11 For reviews on phosphole containing π-conjugated materials see: T. Baumgartner and R. Réau, *Chem. Rev.*, 2006, **106**, 4681–4727; M. G. Hobbs and T. Baumgartner, *Eur. J. Inorg. Chem.*, 2007, 3611–3628.
12 C. Hay, C. Fave, M. Hissler, J. Rault-Berthelot and R. Réau, *Org. Lett.*, 2003, **5**, 3467–3470.
13 H.-C. Su, O. Fadhel, C.-J. Yang, T.-Y. Cho, C. Fave, M. Hissler, C.-C. Wu and R. Réau, *J. Am. Chem. Soc.*, 2006, **128**, 983–995; B. Nohra, Y. Yao, C. Lescop and R. Réau, *Angew. Chem.*, 2007, **119**, 8390–8393 (*Angew. Chem., Int. Ed.*, 2007, **46**, 8242–8245); V. Lemau de Talancé, M. Hissler, L.-Z. Zhang, T. Kárpáti, L. Nyulászi, D. Caras-Quintero, P. Bäuerle and R. Réau, *Chem. Commun.*, 2008, 2200–2202.
14 C. Hay, M. Hissler, C. Fischmeister, J. Rault-Berthelot, L. Toupet, L. Nyulászi and R. Réau, *Chem.–Eur. J.*, 2001, **7**, 4222–4236.
15 C. Fave, M. Hissler, T. Kárpáti, J. Rault-Berthelot, V. Deborde, L. Toupet, L. Nyulászi and R. Réau, *J. Am. Chem. Soc.*, 2004, **126**, 6058–6063; J. Crassous and R. Réau, *Dalton Trans.*, 2008, 6865–6876.
16 C. Hay, C. Fischmeister, M. Hissler, L. Toupet and R. Réau, *Angew. Chem.*, 2000, **112**, 1882–1885 (*Angew. Chem., Int. Ed.*, 2000, **39**, 1812–1815).
17 C. Fave, T.-Y. Cho, M. Hissler, C.-W. Chen, T.-Y. Luh, C.-C. Wu and R. Réau, *J. Am. Chem. Soc.*, 2003, **125**, 9254–9255; M. Sebastian, M. Hissler, C. Fave, J. Rault-Berthelot, C. Odin and R. Réau, *Angew. Chem.*, 2006, **118**, 6298–6301 (*Angew. Chem., Int. Ed.*, 2006, **45**, 6152–6155); W. Shen, S. Graule, J. Crassous, C. Lescop, H. Gornitzka and R. Réau, *Chem. Commun.*, 2008, 850–852; M. Hissler, C. Lescop and R. Réau, *C. R. Chim.*, 2008, **11**, 628–640.
18 C. Hay, D. Le Vilain, V. Deborde, L. Toupet and R. Réau, *Chem. Commun.*, 1999, 345–346; O. Fadhel, M. Gras, N. Lemaitre, V. Deborde, M. Hissler, B. Geffroy and R. Réau, *Adv. Mater.*, 2009, **21**, 1261–1265.
19 M. Sauthier, B. Le Guennic, V. Deborde, L. Toupet, J.-F. Halet and R. Réau, *Angew. Chem.*, 2001, **113**, 234–237 (*Angew. Chem., Int. Ed.*, 2001, **40**, 228–238); C. Hay, M. Sauthier, V. Deborde, M. Hissler, L. Toupet and R. Réau, *J. Organomet. Chem.*, 2002, **643–644**, 494–497; M. Sauthier, F. Leca, L. Toupet and R. Réau,

Organometallics, 2002, **21**, 1591–1602; C. Fave, M. Hissler, K. Sénéchal, I. Ledoux, J. Zyss and R. Réau, *Chem. Commun.*, 2002, 1674–1675; F. Leca, M. Sauthier, V. Deborde, L. Toupet and R. Réau, *Chem.–Eur. J.*, 2003, **9**, 3785–3795; F. Leca, C. Lescop, L. Toupet and R. Réau, *Organometallics*, 2004, **23**, 6191–6201; F. Leca, C. Lescop, E. Rodriguez-Sanz, K. Costuas, J.-F. Halet and R. Réau, *Angew. Chem.*, 2005, **117**, 4436–4439 (*Angew. Chem., Int. Ed.*, 2005, **44**, 4362–4365); F. Leca and R. Réau, *J. Catal.*, 2006, **238**, 425–429; S. Urig, K. Fritz-Wolf, R. Réau, C. Herold-Mende, K. Tóth, E. Davioud-Charvet and K. Becker, *Angew. Chem.*, 2006, **118**, 1915–1920 (*Angew. Chem., Int. Ed.*, 2006, **45**, 1881–1886); B. Nohra, S. Graule, C. Lescop and R. Réau, *J. Am. Chem. Soc.*, 2006, **128**, 3520–3521; B. Nohra, E. Rodriguez-Sanz, C. Lescop and R. Réau, *Chem.–Eur. J.*, 2008, **14**, 3391–3403; S. Welsch, C. Lescop, M. Scheer and R. Réau, *Inorg. Chem.*, 2008, **47**, 8592–8594; S. Welsch, C. Lescop, R. Réau and M. Scheer, *Dalton Trans.*, 2009, 2683–2686; S. Graule, M. Rudolph, N. Vanthuyne, J. Autschbach, C. Roussel, J. Crassous and R. Réau, *J. Am. Chem. Soc.*, 2009, **131**, 3183–3185; S. Welsch, B. Nohra, E. V. Peresypkina, C. Lescop, M. Scheer and R. Réau, *Chem.–Eur. J.*, 2009, **15**, 4685–4703; O. Fadhel, D. Szieberth, V. Deborde, C. Lescop, L. Nyulászi, M. Hissler and R. Réau, *Chem.–Eur. J.*, 2009, **15**, 4914–4924.

20 *Handbook of Oligo- and Polythiophenes*, ed. D. Fichou, Wiley-VCH, Weinheim, 1998 ; I. F. Perepichka, D. F. Perepichka, H. Meng and F. Wudl, *Adv. Mater.*, 2005, **17**, 2281–2305.

21 T. Baumgartner, T. Neumann and B. Wirges, *Angew. Chem.*, 2004, **116**, 6323–6328 (*Angew. Chem., Int. Ed.*, 2004, **43**, 6197–6201); T. Baumgartner, W. Bergmans, T. Kárpáti, T. Neumann, M. Nieger and L. Nyulászi, *Chem.–Eur. J.*, 2005, **11**, 4687–4699; T. Baumgartner and W. Wilk, *Org. Lett.*, 2006, **8**, 503–506; Y. Dienes, S. Durben, T. Kárpáti, T. Neumann, U. Englert, L. Nyulászi and T. Baumgartner, *Chem.–Eur. J.*, 2007, **13**, 7487–7500; S. Durben, D. Nickel, R. A. Krüger, T. C. Sutherland and T. Baumgartner, *J. Polym. Sci., Part A: Polym. Chem.*, 2008, **46**, 8179–8190.

22 S. Durben, Y. Dienes and T. Baumgartner, *Org. Lett.*, 2006, **8**, 5893–5896.

23 C. Romero-Nieto, S. Durben, I. M. Kormos and T. Baumgartner, *Adv. Funct. Mater.*, 2009, **91**, 3625–3631.

24 Y. Dienes, M. Eggenstein, T. Neumann, U. Englert and T. Baumgartner, *Dalton Trans.*, 2006, 1424–1433.

25 T. Neumann, Y. Dienes and T. Baumgartner, *Org. Lett.*, 2006, **8**, 495–497; Y. Dienes, M. Eggenstein, T. Kárpáti, T. C. Sutherland, L. Nyulászi and T. Baumgartner, *Chem.–Eur. J.*, 2008, **14**, 9878–9889; C. Romero-Nieto, S. Merino, J. Rodríguez-López and T. Baumgartner, *Chem.–Eur. J.*, 2009, **15**, 4135–4145; Y. Ren, Y. Dienes, S. Hettel, M. Parvez, B. Hoge and T. Baumgartner, *Organometallics*, 2009, **28**, 734–740; Y. Dienes, U. Englert and T. Baumgartner, *Z. Anorg. Allg. Chem.*, 2009, **635**, 238–244; D. Ren Bai, C. Romero-Nieto and T. Baumgartner, *Dalton Trans.*, 2010, **39**, 1250–1260.

26 R. Streubel, *Coord. Chem. Rev.*, 2002, **227**, 175–192; R. Streubel, *Top. Curr. Chem.*, 2003, **223**, 91–109.

27 H. Helten, M. Engeser, D. Gudat, R. Schilling, G. Schnakenburg, M. Nieger and R. Streubel, *Chem.–Eur. J.*, 2009, **15**, 2602–2616.

28 This method could also be applied for the synthesis of other heterocyclic compounds: H. Helten, G. von Frantzius, G. Schnakenburg, J. Daniels and R. Streubel, *Eur. J. Inorg. Chem.*, 2009, 2062–2065; H. Helten, J. Marinas Pérez, J. Daniels and R. Streubel, *Organometallics*, 2009, **28**, 1221–1226; S. Fankel, H. Helten, G. von Frantzius, G. Schnakenburg, J. Daniels, V. Chu, C. Müller and R. Streubel, *Dalton Trans.*, 2010, **39**, 3472–3481.

29 H. Helten, C. Neumann, A. Espinosa, P. G. Jones, M. Nieger and R. Streubel, *Eur. J. Inorg. Chem.*, 2007, 4669–4678.

30 S.-A. Chen and G.-W. Hwang, *Macromolecules*, 1996, **29**, 3950–3955; Y. Liu and M. Liu, *Thin Solid Films*, 2002, **415**, 248–252.

31 R. Streubel, S. Priemer, F. Ruthe, P. G. Jones and D. Gudat, *Eur. J. Inorg. Chem.*, 1998, 575–578.

32 G. Barbarella, M. Zambianchi, L. Antolini, P. Ostoja, P. Maccagnani, A. Bongini, E. A. Marseglia, E. Tedesco, G. Gigli and R. Cingolani, *J. Am.Chem. Soc.*, 1999, **121**, 8920–8926.

33 F. H. Allen, O. Kennard, D. G. Watson, L. Brammer, A. G. Orpen and R. Taylor, *J. Chem. Soc., Perkin Trans. 2*, 1987, S1–S19.

34 H. Weiss, R. Ahlrichs and M. Häser, *J. Chem. Phys.*, 1993, **99**, 1262–1270; R. Bauernschmitt and R. Ahlrichs, *J. Chem. Phys.*, 1996, **104**, 9047–9052; R. Bauernschmitt and R. Ahlrichs, *Chem. Phys. Lett.*, 1996, **256**, 454–464.

35 R. Bauernschmitt and R. Ahlrichs, *Chem. Phys. Lett.*, 1996, **256**, 454–464.

36 G. M. Sheldrick, *Acta Crystallogr., Sect. A: Fundam. Crystallogr.*, 2008, **64**, 112–122.

37 R. Ahlrichs, M. Bär, M. Häser, H. Horn and C. Kölmel, *Chem. Phys. Lett.*, 1989, **162**, 165–169.

38 M. v. Arnim and R. Ahlrichs, *J. Chem. Phys.*, 1999, **111**, 9183–9190.

39 A. D. Becke, *Phys. Rev. A*, 1988, **38**, 3098–3100.

40 C. Lee, W. Yang and R. G. Parr, *Phys. Rev. B: Condens. Matter*, 1988, **37**, 785–789.

41 K. Eichkorn, O. Treutler, H. Öhm, M. Häser and R. Ahlrichs, *Chem. Phys. Lett.*, 1995, **240**, 283–290; K. Eichkorn, O. Treutler, H. Öhm, M. Häser and R. Ahlrichs, *Chem. Phys. Lett.*, 1995, **242**, 652–660; K. Eichkorn, F. Weigend, O. Treutler and R. Ahlrichs, *Theor. Chem. Acc.*, 1997, **97**, 119–124.

42 A. Schäfer, H. Horn and R. Ahlrichs, *J. Chem. Phys.*, 1992, **97**, 2571–2577.

43 D. Andrae, U. Häußermann, M. Dolg, H. Stoll and H. Preuß, *Theor. Chim. Acta*, 1990, **77**, 123–141.

44 P. Deglmann, F. Furche and R. Ahlrichs, *Chem. Phys. Lett.*, 2002, **362**, 511–518; P. Deglmann and F. Furche, *J. Chem. Phys.*, 2002, **117**, 9535–9538; P. Deglmann, K. May, F. Furche and R. Ahlrichs, *Chem. Phys. Lett.*, 2004, **384**, 103–107.

45 A. D. Becke, *J. Chem. Phys.*, 1993, **98**, 5648–5652.

